Determining surface orientations of specular surfaces by intensity encoded illumination

Shree K. Nayar and Arthur C. Sanderson

Carnegie Mellon University, Department of Electrical and Computer Engineering and The Robotics Institute
Pittsburgh, Pennsylvania 15213

ABSTRACT

This paper discusses an intensity encoded line source illumination approach to estimating the surface orientation of specular surfaces. The normalized brightness difference function (NBDF) is introduced as a real time invertible relationship between image irradiances and surface orientation, and provides the basis for estimation of the surface gradient using relative brightness values rather than calibrated photometric measurements. Two complementary line source intensity patterns are generated for each measurement, and a series of radial lines are scanned to span the surface gradient space. A brief analysis of the sensitivity of estimation to the sharpness of specularity is conducted. Experiments have estimated the accuracy of the orientation measurement to be within 2-3%. Sensitivity to variations in specularity, and the feasibility of the encoding technique are described. Careful attention to the illumination geometry, distant source approximation and computation speed will be required for the purpose of practical implementation. The use of line sources is most suited to applications where the relevant features can be extracted from a finite set of cross sections of the object. Inspection of solder and machined metal are examples of the application of intensity encoding.

1. INTRODUCTION

For diffuse surfaces, surface radiance is a smoothly varying, though sometimes complex function of the incidence and the viewing angle. However, using multiple sources positioned in different source directions, the resulting image irradiances may be used to determine surface orientation, as in the case of photometric stereo [7,8]. When the position and the orientation of a single light source and camera as well as the reflectivity function of the surface are accurately known, the shape from shading technique [4] may be used, to iteratively compute surface orientations that minimize errors in image intensities under carefully selected smoothness constraints with orientations at the occluding contours used as boundary conditions.

In this paper we concentrate on specular or shiny surfaces. Such shiny objects are common in manufacturing and therefore of particular interest for inspection and robotic manipulation applications. For specular reflection, the angle of reflection equals the angle of incidence and both rays and the surface normal lie in the same plane. Image irradiances, therefore, become very strong functions of the viewing angle. If the surface is purely specular its reflectivity is represented by a double delta function [1]. It is therefore evident that under the distant source assumption, for a orthonormal camera model and a single source, the bright points in the image correspond to surface elements having the same orientation. In order to span the complete gradient space an infinite number of source positions would be necessary. An inexpensive method for extracting shape information of shiny objects, is thus desirable.

A source intensity encoding approach is proposed in this paper, as a method of relating image irradiances to source positions without prior knowledge of the surface albedo or absolute illumination intensities. A single fixed camera determines the viewing angle and line sources are arranged around the origin centered object. Two images resulting from complementary intensity patterns on each line source, are used to compute the surface orientations. Each of the two patterns on the line source is generated by a point source. The two image irradiance values at the same point on the surface, map a unique physical point on the line source to that point on the surface. The estimation of the surface orientation at each point thereafter, is straightforward.

2. BACKGROUND

Orientation of a physical surface element at any point (x,y) in the image plane can be expressed in terms of p and q, the two orthogonal components that constitute the gradient space [1]. It is convenient to superimpose the p and q axes on the x and y image plane coordinate axes, so that a surface patch with orientation (p,q) has the surface normal vector (-p,-q,1) in the viewer oriented frame[1]. A reflectance map R(p,q) [1,7] is utilized to describe the relationship between image irradiance R and the surface orientation (p,q). Given the direction and intensity of surface illumination, the surface normal and the reflectance properties of the surface, the brightness E(x,y) of the surface element in the image can be determined as,

$$E(x,y) = R\{p(x,y),q(x,y)\}. \quad (1)$$

Since the above expression cannot be inverted to obtain a unique orientation (p,q) from a single image E(x,y), the basic photometric stereo [4] approach uses multiple images produced by multiple sources.

Specular surfaces such as mirrors and polished metal, reflect light only at an angle of reflection e equal to the angle of incidence i and in a direction such that the incident unit vector s, the normal unit vector n and the viewing or emittance unit vector z, are coplanar. In order to register reflections or highlights in the image from surface elements of all orientations, multiple planar(extended) sources, each with an intensity gradient, were used by Ikeuchi [5] to illuminate the surface. Though multiple planar sources make the inversion of equation (1) possible, the computation involved is substantial since the recursive Newton method was used to solve the non linear form of equation (1).

Without prior knowledge of the intensity function on the planar sources, the reflectance map in the form of a look-up table may be built up by recording for each of three planar sources the brightness value reflected off a hemisphere of known surface geometry and reflectance characteristics similar to that of the surface of interest. Under the assumption of distant sources, known object position and an orthonormal camera model, three brightness values $E_1(x,y)$, $E_2(x,y)$ and $E_3(x,y)$ are measured at each point (x,y) on the sphere. The three image irradiances are normalized in order to eliminate the effects of the illumination intensities I and surface albedo p. Each normalized set $\{e_1,e_2,e_3,\}$ corresponds to the known orientation (p,q) at the point (x,y) on the hemisphere [5]. The range of orientations on the hemisphere, that produce reflections in the image from all three planar sources, is small. By using additional sources at appropriate positions around the object and by increasing the dimensions of the reflectance map, a larger range of orientations can be accommodated. The intensity encoding technique in this paper is closely related to

this approach, but employs a line source and complementary intensity patterns to simplify the calibration and measurement problems.

Sanderson et al [6] have demonstrated the structured highlight technique for determining specular surface orientations. The object is centered at the origin and an array of point sources are positioned around the object. All reflected highlights are viewed by a single camera. When the source is distant from the object as compared to the distance of all surface elements from the origin, the vector s in the source direction is independent of the position of the surface element. The array of point sources $\{S_k; k = 1,2,...,N\}$, each with the spherical coordinates (r_k,θ_k,ϕ_k) is scanned, and the resulting image $E_k(x,y)$ is thresholded to generate points $h_k(x,y)$ in the image that correspond to highlights or specular peaks. For a source direction $(p(\theta_k,\phi_k), q(\theta_k,\phi_k))$ in the gradient space the specular peaks occur at surface points with the orientation $(p(\theta_k,\phi_k/2), q(\theta_k,\phi_k/2))$, as shown in Fig.(1). Experimental results from SHINY system for structured highlight inspection are described in [6] and illustrate reliable mapping of surface contours for specular surfaces.

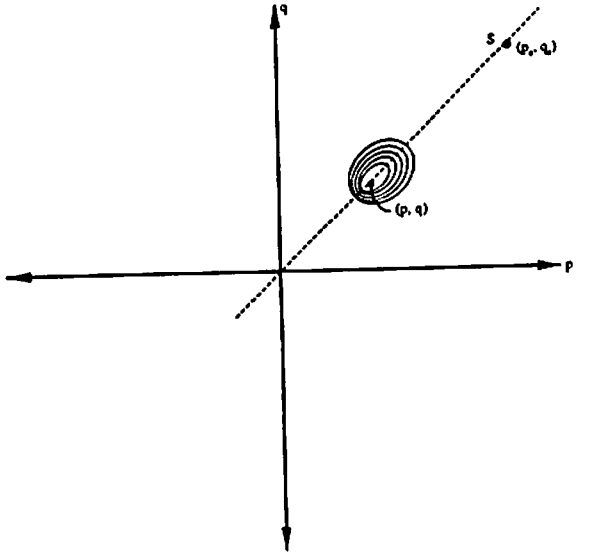

Figure 1. Reflectance map for a distant point source and a specular surface. Equal brightness contours represent the sharp specular peak.

3. INTENSITY ENCODING

In the intensity encoding approach to determining surface orientation of specular surfaces, two different intensity profiles are generated for each line source position, and the ratio of the brightness values at any point in the image determines the corresponding point on the line source and therefore the local surface gradient. Each source direction and viewing direction corresponds to a unique local surface normal. This method differs from photometric stereo, in that, the relationship between image irradiances and surface orientation (p,q) is derived from the geometries of illumination and imaging as an easily invertible function, thus avoiding the iterative off line generation of a reflectance map in the form of a look up table. The line source geometry and the choice of complementary illumination patterns makes this possible. As in the case of structured highlight inspection, an array of line sources is scanned in order to span values of the azimuth component θ of the surface orientation. However, in comparing the proposed method with the structured highlight approach it may be noted that each line source represents an infinite

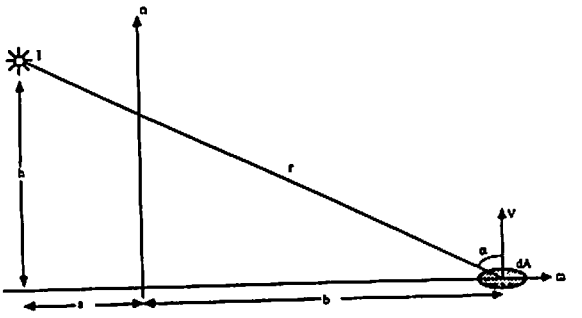

Figure 2. Illumination of a surface by a point source.

set of encoded point sources. In many applications one or more profiles or cross sections of an object are of particular interest, in which case line sources are ideal.

Consider the point source in Fig.(2) with a radiant intensity I, making an angle α with the surface normal v at the point b on the object surface. The irradiance E(b) of the surface at the point b is expressed as,

$$E(b) = \frac{I\cos\alpha}{r^2}. \qquad (2)$$

By using the geometry shown in Fig.(2), the above expression can be written in the form:

$$E(b) = \frac{Ih}{(h^2+(a+b)^2)^{3/2}}. \qquad (3)$$

The relative positions and orientations of the point sources, the line source, the centered object, and the camera are shown in Fig.(3).

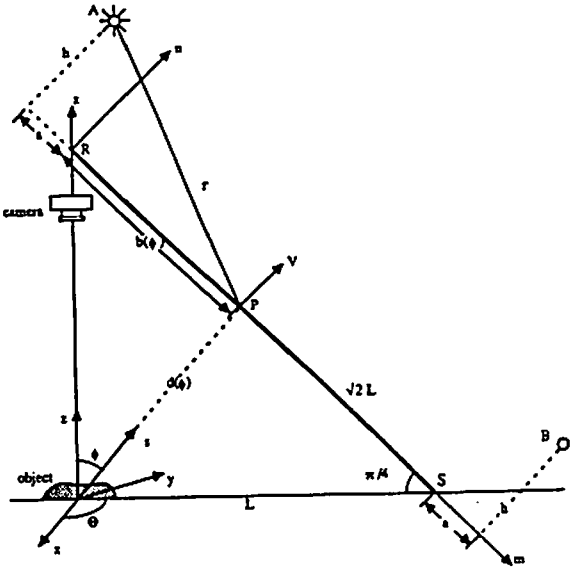

Figure 3. Illumination and imaging geometries that define the relative positions and orientations of the point sources, line source, object, and the camera.

The line source RS is a diffusion plate, that is illuminated by one of the two point sources A and B. The Lambertian properties of the line source diffuse incident light such that each point on RS has a radiance that is independent of direction. The radiance of the line source at the point b in the direction of the object is given by,

$$L_d(\phi) = (1-K)\, E(b(\phi)) \tag{4}$$

where K represents an unknown fraction of energy that is wasted in the diffusion process, and ϕ is the colatitude component of the source direction.

For the purpose of discussion, we shall assume that the inspected surface is purely specular, in which case the Bidirectional Reflectance Distribution Function (BRDF) [1] is a double delta function. The results will be extended to a more general and realistic model of specular reflectance. For a purely specular model, the reflected radiance L_r of a surface patch in the direction of reflection is simply the incident radiance L_d in the corresponding reflected direction. Let us assume, that light from the point $b(\phi)$ on the line source is reflected by the specular surface to the point (x,y) on the image plane. The imaging geometry allows only one physical point on the surface to contribute to the image irradiance at a particular point in the image. Therefore, the image irradiance E(x,y) at the image point (x,y) is related to the incident radiance $L_d(\phi)$ as,

$$E(x,y) = A\, L_d(\phi) \tag{5}$$

where A is a constant related to surface albedo and the distance between the object and the camera. The above relationship is linear since an orthographic projection of the object makes the image irradiances independent of the position of the surface element in the image. By using the previous relations, the above expression can be written as,

$$E(x,y) = \frac{IA(1-K)h}{(h^2+(a+b(\phi))^2)^{3/2}} \tag{6}$$

It is seen from Fig.(3) that a non zero value of image irradiance at a point (x,y) has two implications. The first is that the azimuth angle θ_n of the surface orientation at the point (x,y), equals the azimuth angle θ of the line source. Secondly, the colatitude angle ϕ_n of the surface orientation at the point (x,y) is bounded by the limits 0 and $\pi/4$ radians since the colatitude angle ϕ of any point on the line source lies between 0 and $\pi/2$ radians. Fig.(4) shows the image irradiance plotted as a function of ϕ for a given illumination geometry defined by a, h, and L, and the product IA(1-K) equal to unity.

Consider the source radiances $L_{dA}(\phi)$ and $L_{dB}(\phi)$ at the point $b(\phi)$ and in the source direction ϕ, generated by the point sources A and B respectively. The resulting image irradiances E_A and E_B at the image point (x,y), are recorded. At this point we define the Normalized Brightness Difference function (NBDF) as,

$$D(x,y) = \frac{E_A(x,y) - E_B(x,y)}{E_A(x,y) + E_B(x,y)} \quad \text{for,} \tag{7}$$

$$E_A(x,y) + E_B(x,y) > T.$$

where D(x,y) is the NBDF at the image point (x,y), and the threshold T is chosen so that any point that does not satisfy the above condition is not specular enough and the surface orientation at that point will not be estimated. The two point sources A and B are generated by two fiber optic cables connected to the same primary source, and therefore the ratio of their intensities may be assumed to be constant and insensitive to variations in the intensity of the primary source. By using fiber optic cables of equal length and cross sectional diameter,

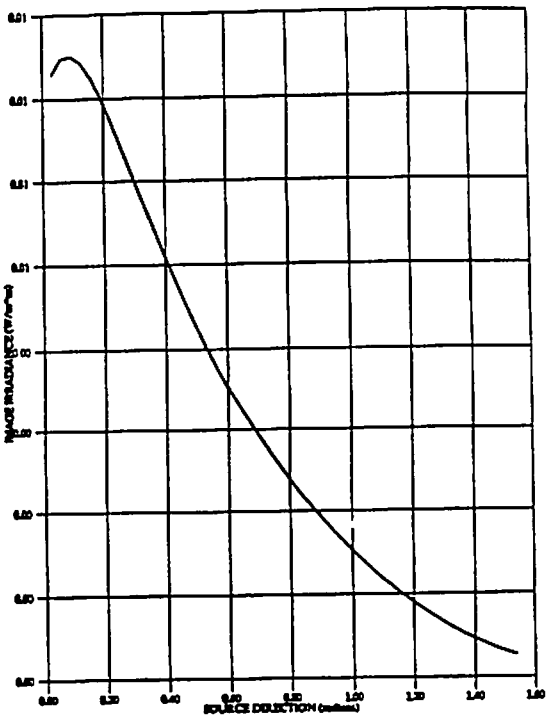

Figure 4. Image irradiance E(x,y) plotted as a function of the source direction ϕ for the geometry illustrated in Fig.(3).

the intensity ratio can be adjusted to unity. The intensity profile corresponding to the point source A is generated by physically blocking out the light from source B and vice versa. The symmetry in the illumination geometry shown in Fig.(3) results in an NBDF of the form:

$$D(x,y) = \frac{\dfrac{h}{(h^2+(a+b(\phi))^2)^{3/2}} - \dfrac{h}{(h^2+(a+\sqrt{2}L-b(\phi))^2)^{3/2}}}{\dfrac{h}{(h^2+(a+b(\phi))^2)^{3/2}} + \dfrac{h}{(h^2+(a+\sqrt{2}L-b(\phi))^2)^{3/2}}} \tag{8}$$

where D(x,y) is independent of surface albedo, the radiant intensities of sources A and B, and the distances of the object from the line source and the camera. The NBDF is made an increasing function of $b(\phi)$ by selecting values of a and h that force the first derivative of D with respect to $b(\phi)$ to be positive in the interval $0 \leq b(\phi) \leq \sqrt{2}L$. The use of complementary illumination patterns by the symmetrical placement of point sources on either side of the line source, simplifies the selection of a and h. Since image irradiance values are positive, equation (8) implies:

$$|D(x,y)| \leq 1. \tag{9}$$

The final step involves the inversion of equation (8) to obtain a unique source point corresponding to a given NBD value D, at the image point (x,y). By simply expanding equation (8) we obtain an equivalent expression of the form:

$$b(\phi)^2 (1-G) + b(\phi)\,(2a+2\sqrt{2}LG+2aG) + (h^2+a^2-h^2G-a^2G-2L^2G-2\sqrt{2}LaG) = 0 \tag{10}$$

where

$$G = \left(\frac{1-D(x,y)}{1+D(x,y)}\right)^{2/3}.$$

The above relationship yields two solutions to $b(\phi)$ in terms of $D(x,y)$ and the constants a, h, and L of the illumination geometry. However only one of the solutions lies in the range $0 \leq b(\phi) \leq \sqrt{2}L$ and therefore is valid. Given the source position $b(\phi)$, the source direction is obtained from Fig.(3) as:

$$\phi = \tan^{-1}\left(\frac{b(\phi)}{\sqrt{2}L - b(\phi)}\right) \tag{11}$$

On the basis of the above relations, the estimation of surface orientation by intensity encoding can be summarized as follows: Given the image irradiances $E_A(x,y)$ and $E_B(x,y)$ we find the corresponding NBD, $D(x,y)$. Each $D(x,y)$ corresponds to a unique source direction with the polar angle (θ,ϕ) where θ is determined by the azimuth angle of the line source under consideration and ϕ is determined by equations (10) and (11). Hence the source orientation (p_s,q_s) in the gradient space is determined [1] by the equations,

$$p_s = -\cos\theta\tan\phi, \tag{12}$$

$$q_s = -\sin\theta\tan\phi.$$

As illustrated in Fig.(1), in the case of a specular surfaces the corresponding specular peaks occur at surface patches with the orientation (p,q) where,

$$p = p_s\left([1+p_s^2+q_s^2]^{1/2} - 1\right)/(p_s^2+q_s^2), \tag{13}$$

$$q = q_s\left([1+p_s^2+q_s^2]^{1/2} - 1\right)/(p_s^2+q_s^2).$$

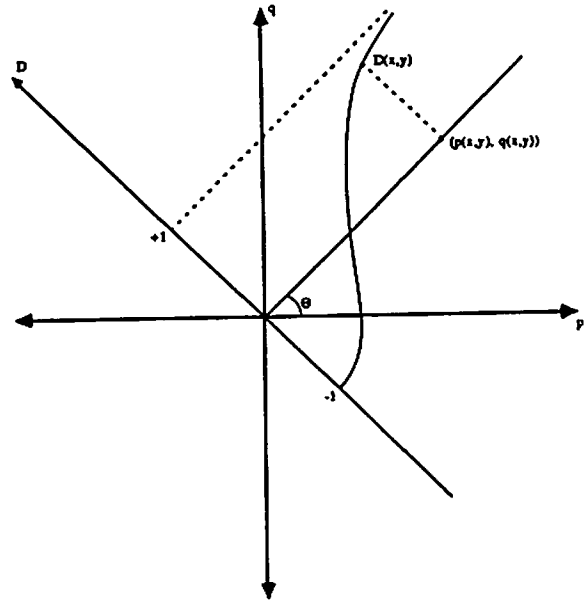

Figure 5. Reflectance map for a single line source. Each Normalized Brightness Difference value corresponds to a unique surface orientation.

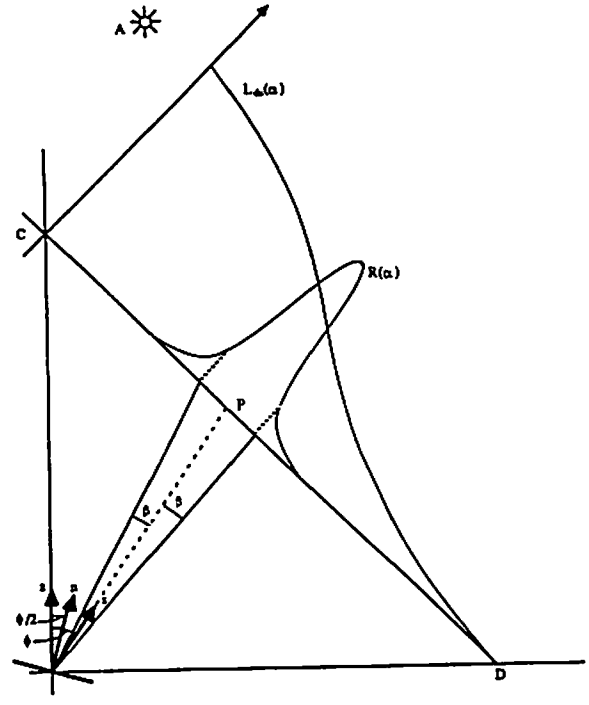

Figure 6. A realistic specular model where the image irradiance at each point in the image is a weighted contribution of points in a small section of the line source.

A reflectance map representation of the surface orientation (p,q) as a function of the NBDF $D(x,y)$ for a single line source position θ, is shown in Fig.(5).

We conclude this section with a brief note on the sensitivity of the normalized brightness function to the sharpness of specularity, n. For a non-ideal specular surface, one may consider a model where all the points in the small neighborhood $\phi-\beta \leq \alpha \leq \phi+\beta$ of the point source $P(\theta,\phi)$, contribute to the image irradiance at points with a normal vector in the direction $(\theta,\phi/2)$, as shown in Fig.(6). By modifying equation (6), the image irradiance resulting from the point source A is given by:

$$E_A(x,y) = C\int_{\phi-\beta}^{\phi+\beta} L_{dA}(\alpha)\, R(\alpha)\, d\alpha \tag{14}$$

where C is a constant and $R(\alpha)$ represents the reflectance characteristics of the surface and is symmetrical about $\alpha = \phi$ when the Lambertian component is negligible. In the case of very shiny objects, $R(\alpha)$ has a sharp peak and thus it is reasonable to assume that $L_{dA}(\alpha) = L_{dA}(\phi)$ for $\phi-\beta \leq \alpha \leq \phi+\beta$ and the above expression can be rewritten as:

$$E_A(x,y) = C\, L_{dA}(\phi)\int_{\phi-\beta}^{\phi+\beta} R(\alpha)\, d(\alpha). \tag{15}$$

The above integral is an approximation of the area under $R(\alpha)$. As the surface orientation that is being estimated varies, the peak in $R(\alpha)$ shifts and is always centered at the source point on the line source that has a colatitude angle twice that of the surface normal vector. Consequently, the integral is a constant and from equations (7) and (8) it is seen that the NBDF $D(x,y)$ is unaffected and is equal to that for a purely specular surface.

A set of line sources $\{LS_k; k = 1,2,....,N\}$ is positioned around the object at the azimuth angles θ_k. Each source LS_k determines surface orientations in the direction (θ_k,ϕ), where $0 \leq \phi \leq \pi/4$. The reflectance map for the complete array of line sources is shown in Fig.(7), where the circles represent the constant NBDF contours.

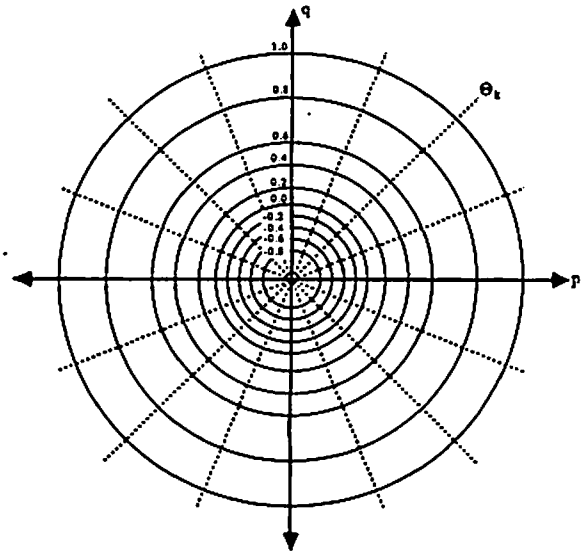

Figure 7. Reflectance map for the complete array of line sources. The concentric circles represent constant NBDF contours and each dotted line corresponds to a single line source.

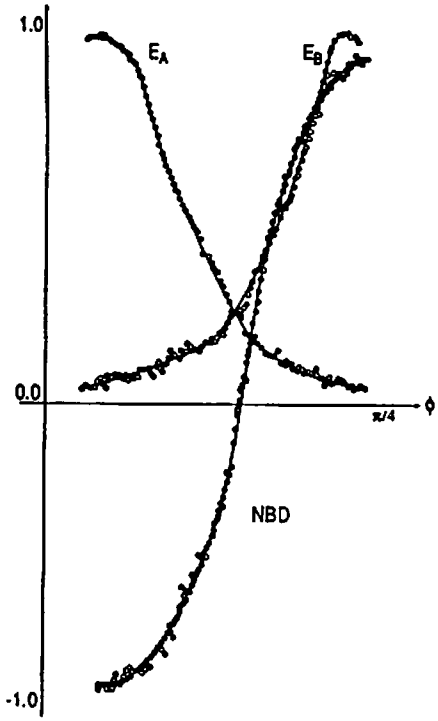

Figure 8. Image irradiances E_A and E_B plotted as a function of ϕ, by reflecting the line source radiance off the surface of a specular sphere. The resulting NBD function D is piecewise approximated by third degree polynomials.

4. EXPERIMENTS

The intensity encoding technique was used to determine the shape of different shiny surfaces. For a given geometry of light sources, the image irradiances E_A an E_B and the corresponding NBDF function were plotted as a function of the source direction ϕ, by using a sphere of known geometry to reflect the source radiances. As seen in Fig.(8) and Fig.(4), E_A and E_B are well approximated by their analytical form and hence with careful implementation a calibration procedure may be avoided.

In order to test the feasibility of the method, experiments were conducted using the POPEYE vision system based on a SUN workstation. The experimental apparatus consists of a Panasonic CCD television camera and a 5 inch long and 0.5 inch wide tracing paper that is used as the diffusing line source. Point sources A and B are generated by two 20 inch long and 0.25 inch diameter flexible fiber optic cables that are illuminated by the same halogen lamp. The line source is exposed to either point source A or B by the use of mechanical shutters fixed at the outlets of sources A and B.

The measurement accuracy was estimated by determining surface orientation at different points on a polished sphere of 0.125 inch diameter. The images corresponding to sources A and B for a single position of the line source, are shown in Fig.(9). A gamma correction is applied to each image irradiance in order to account for the non linear relationship between image irradiance and the corresponding TV camera output. The surface normal vectors were calculated by using the predetermined NBD function. The normal vectors were superimposed on a profile image of the sphere and the vectors were extrapolated, as shown in Fig.(10). A 2-3% accuracy in the

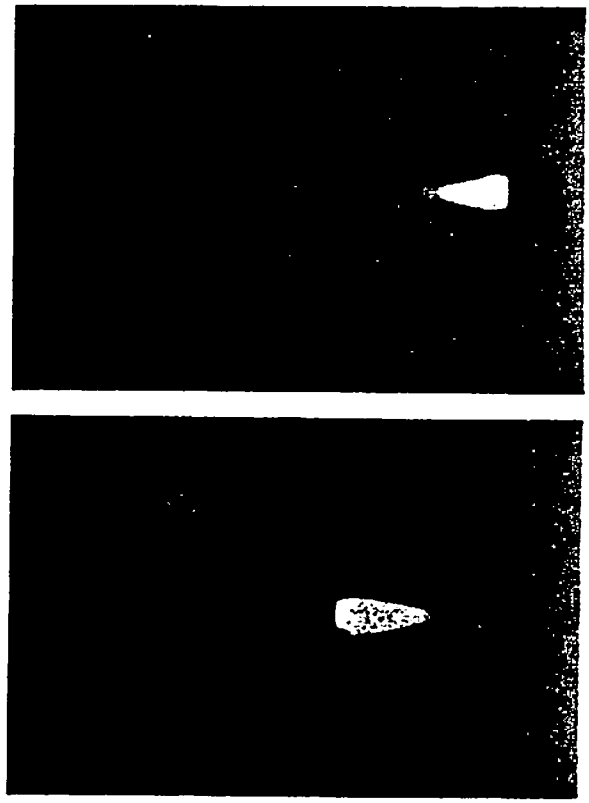

Figure 9. Photos of images of a sphere generated by the point sources A and B for a single line source.

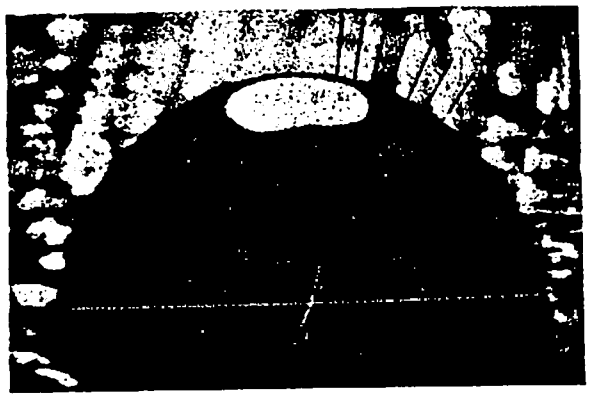

Figure 10. Photo of the estimated normal vectors, overlaid on the profile of the sphere. The proximity of the point of intersection of the extended vectors to the center of the sphere, determines the accuracy of the intensity encoding method.

orientation determination is estimated, based on the intersection of the extended normals at the centre of the sphere. Fig.(11a) shows the side view of a solder joint for a surface mounted component on a circuit board. The measured normal vectors and the reconstructed profile of a solder joint, for a single line source position, are overlaid on a gray-level image of the solder joint as shown in Fig.(11b). The shape of the reconstructed profile provides information on the quality of the joint. The surface in this case has a sharpness of specularity less than that of the sphere, however, the reconstructed profile was found to be accurate.

The overall accuracy of the encoding approach is dependent on the noise level in the brightness images, the relative weighting of the Lambertian and specular components of the surface reflectance, and the distant source approximation. Given the source and camera positions, the normal vector may be determined by the use of a perspective or an orthonormal model. In our implementation it was found that the geometry of the point sources and the line sources with respect to the object and the viewing direction, need be known only with an accuracy of 5%.

5. CONCLUSION

In this paper we have described the use of intensity encoding of light sources, for the estimation of the surface orientation of specular objects. Intensity encoding is based on the knowledge of the illumination and imaging geometries. We have defined the Normalized Brightness Difference function as a real time invertible function, that relates two image irradiances to a unique surface orientation. Experiments have been conducted on surfaces with different degrees of specularity and a 2-3% accuracy in orientation measurement is estimated. Intensity encoding does not require calibration such as that typically used by photometric methods. It has the inherent advantage of speed over the structured highlight approach, since each line source represents a set of point sources that need to be independently scanned in the case of structured highlight.

The factors affecting practical implementation of intensity encoding are the noise levels in the imaging system, relatively large objects that violate distant source approximation, an accurate estimation of illumination and imaging geometries, and the effect of ambient lighting in the area of operation. The method is most suited for the inspection of small shiny objects, in which case line sources can be accurately positioned around the object and the effects of external lighting minimized.

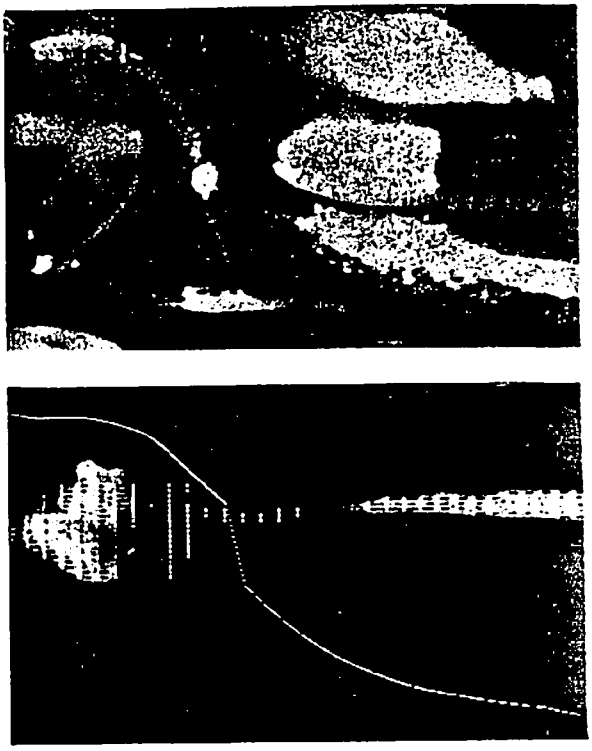

Figure 11. (a). Side view of a solder joint on a circuit board. (b). Photo of the orientation map for a single line source and the reconstructed profile superimposed on a gray-level image of the solder joint.

REFERENCES

1. B. K. P. Horn and R. W. Sjoberg, "Calculating the reflectance map," *Applied Optics*, Vol. 18, No. 1, pp. 1770-1779.
2. B. K. P. Horn, "Determining shape from shading," in *The Psychology of Computer Vision*, P. H. Winston, Ed. New York: McGraw-Hill, 1975.
3. B. K. P. Horn, "Image intensity understanding," *Artificial Intelligence*, Vol. 8, No. 2, 1977.
4. K. Ikeuchi, "Numerical shape from shading and occluding contours in a single view," Artificial Intelligence Lab., MIT, Cambridge, AI-Memo 566, 1980.
5. K. Ikeuchi, "Determining surface orientations of specular surfaces by using the photometric stereo method," IEEE Trans. PAMI, Vol. PAMI-3, No. 6, pp. 661-669, November, 1981.
6. A. C. Sanderson, L. E. Weiss, S. K. Nayar,"Structured Highlight Inspection of specular surfaces," in press, IEEE Trans. PAMI.
7. R. J. Woodham, "Photometric stereo: A reflectance map technique for determining surface orientation from image intensity," Proc. SPIE, vol. 155, pp. 136-143, 1978.
8. R. J. Woodham, "Photometric method for determining surface orientation from multiple images," *Optical Engineering*, Vol. 19, No. 1, pp. 139-144, 1980.